Critical Opacity: A Possible Explanation of the Fast Thermalization Times Seen in BNL RHIC Experiments

F. Gastineau, E. Blanquier, and J. Aichelin

SUBATECH, Laboratoire de Physique Subatomique et des Technologies Associées, University of Nantes-IN2P3/CNRS-Ecole des Mines de Nantes, 4 rue Alfred Kastler, F-44072 Nantes, CEDEX 03, France

(Received 25 March 2004; published 27 July 2005)

The Nambu–Jona-Lasinio Lagrangian offers an explication of the seemingly contradictory observations that (a) the energy loss in the entrance channel of heavy ion reactions is not sufficient to thermalize the system and that (b) the observed hadron cross sections are in almost perfect agreement with hydrodynamical calculations. According to this scenario, a critical opacity develops close to the chiral phase transition which equilibrates and hadronizes the expanding system very effectively. It creates as well radial flow and, if the system is not isotropic, finite v_2 values.

DOI: 10.1103/PhysRevLett.95.052001 PACS numbers: 12.38-t, 25.75-q

Introduction.—Some of the most surprising results of the ongoing BNL RHIC experiments are the large radial flow $\beta_{\mathrm{rad}} \approx 0.5$, the large v_2 values, where v_2 is the second Fourier coefficient of a Fourier expansion in ϕ_p of $dN/(dy p_t dp_t d\phi_p)$, and the fact that hydrodynamical models describe not only the total but also the differential anisotropy $v_2(p_t)$ up to a transverse momentum of $p_t = 2$ GeV [1–5]. The initial energy densities, at $\tau = 1$ fm/c, employed in these calculation are between 4 and 6 GeV/fm^3 and agree quite well with the Bjorken estimate [6]. This seems to indicate that the system is at that time close to local equilibrium. For a survey of the results of the hydrodynamical approaches, see [7]. The problem with these findings is that one does not understand how the system comes so fast to equilibrium. The energy loss of incoming partons is of the order of 1 GeV/fm [8,9]. Independent of the reaction scenario employed (minijets [10] or Weizsaecker-William fields of the incoming nuclei which materialize into on-shell gluons [11]), the time needed for equilibration is much longer. For a recent review, see [12].

All these models share the feature that at energies below the validity of perturbative QCD (PQCD) phenomenological approaches have to be employed. Therefore it may be worthwhile to use another phenomenological model which has been shown to be quite successful in regions where it can be compared with QCD, the Nambu–Jona-Lasinio (NJL) model [13,14]. Supplemented by a 't Hooft determinant the NJL Lagrangian has the same symmetries as the QCD Lagrangian, which are known to be the basis of many properties of quark and hadronic matter. It predicts [15], as PQCD [16,17] calculations, color flavor locking at low temperatures and high densities, allows one to describe the meson masses at low density and low temperature [14], and provides a simple approach to study the chiral phase transition. It predicts as well the tricritical point in the ρ-T phase diagram which has recently been predicted by lattice QCD calculations [18]. Of course this model has its deficiencies as well: Based on a local four-fermion interaction it is not renormalizable, and therefore a cutoff Λ has to be employed to regularize the loops. Furthermore, due to the locality of the interaction, confinement is not present and gluons do not appear as degrees of freedom. Because of these drawbacks, it is hard to judge the quantitative prediction of this model, but it can certainly serve for qualitative studies.

Using this model, we will show that due to the interplay between the quark and meson masses close to the chiral phase transition the system may develop a critical opacity where all s-channel transition rates become very large. This it true for the elastic as well as for the hadronization cross sections. These large cross sections equilibrate very efficiently the expanding plasma and create a gas of mesons although confinement is absent in the NJL Lagrangian. Since the equilibration takes place during the expansion, a strong radial flow develops, which is seen in the data and which is as well not understood yet.

The NJL approach.—The NJL model is the simplest low energy approximation of QCD. It describes the interaction between two quark currents as a pointlike exchange of a perturbative gluon [13]. This local interaction is given by

$$\mathcal{L}^{\mathrm{int}} = \kappa \sum_{c=1}^{N_c^2-1} \sum_{i,j}^{3} (\bar{q}_{i,\alpha}[\gamma_\mu \lambda^c]_{\alpha\delta} q_{i,\delta})(\bar{q}_{j,\gamma}[\gamma^\mu \lambda^c]_{\gamma\beta} q_{j,\beta}), \tag{1}$$

where we have explicitly shown the flavor (i, j) and color or Dirac (α, β, γ, δ) indices. We normalize $\Sigma_{i=0}^{8} \lambda^i_{\alpha\beta} \lambda^i_{\beta\alpha} = 2$. Applying a Fierz transformation in color space to this interaction, the Lagrangian separates into two pieces: an attractive color singlet interaction between a quark and an antiquark ($\mathcal{L}_{(\bar{q}q)}$) and a repulsive color antitriplet interaction between two quarks $\mathcal{L}_{(qq)}$, which disappears in the large N_c limit. Here we are interested only in the color singlet channel (the color octet channel gives diquarks and can be used to study baryons

[15]):

$$\mathcal{L} = \mathcal{L}_0 + \mathcal{L}_{(\bar{q}q)} + \mathcal{L}_A, \tag{2}$$

where $\mathcal{L}_0$ is the free kinetic part. Concentrating on the dominant scalar and pseudoscalar part in Dirac space, we find the following Lagrangian which we use here:

$$\mathcal{L} = \sum_{f=\{u,d,s\}} \Big[\bar{q}_f (i\partial\!\!\!/ - m_{0f}) q_f + G_S \sum_{a=0}^{8} [(\bar{q}_f \lambda_F^a q_f)^2 + (\bar{q}_f i\gamma_5 \lambda_F^a q_f)^2] \Big] + G_D \{\det[\bar{q}_f (1 - i\gamma_5) q_f] + \det[\bar{q}_f (1 + i\gamma_5) q_f]\}. \tag{3}$$

The first term is the free kinetic part, including the flavor dependent current quark masses m_{0f} which explicitly break the chiral symmetry of the Lagrangian. The second part is the scalar-pseudoscalar interaction in the mesonic channel. It is diagonal in color. We have added the six point interaction in the form of the 't Hooft determinant which explicitly breaks the $U_A(1)$ symmetry of the Lagrangian. The determinate runs over the flavor degrees of freedom; consequently the flavors become connected.

The model contains five parameters: the current mass of the light and strange quarks, the coupling constants G_D and G_S, and the momentum cutoff Λ. They are fixed by physical observables: the pion and kaon mass, the pion decay constant, the scalar quark condensate $\langle \bar{q}q \rangle$, and the mass difference between η and η'. We will employ the following parameter set: $m_q^0 = 4.75$ MeV, $m_s^0 = 147$ MeV, $G_S/\Lambda^2 = 1.922$, $G_D/\Lambda^5 = 10$, and $\Lambda = 708$ MeV.

The temperature and density dependent masses of the quarks are obtained by reducing the above Lagrangian to a one particle Lagrangian by contracting the remaining field operators in all possible ways. The meson masses are obtained by solving the Bethe Salpeter equation in the $q\bar{q}$ channel. The details of both calculations are found in Ref. [14]. With these parameters, we obtain the meson and quark masses displayed in Fig. 1.

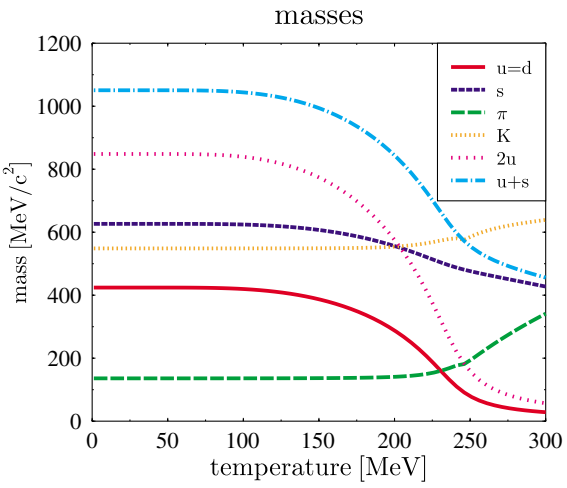

FIG. 1 (color online). Masses of the pseudoscalar mesons and of the quarks in the NJL approach.

Cross sections.—If created in heavy ion collisions, the quark gluon plasma will expand rapidly. Therefore, not the static properties of the theory but the cross sections between constituents become dominant. In the NJL model these cross sections can be calculated via a $1/N_c$ expansion [19,20].

We start out with the elastic cross sections. The $qq \to qq$ cross section has no s-channel contribution and is of the order of some millibarn. It is not important for the phenomena discussed in this Letter. The Feynman diagrams for the $q\bar{q} \to q\bar{q}$ cross section is shown in Fig. 2. The matrix elements in the t and the s channel are given by

$$-i\mathcal{M}_t = \delta_{c_1,c_3}\delta_{c_2,c_4}\bar{u}(p_3)Tu(p_1)[i\mathcal{D}_t^S(p_1 - p_3)] \times v(p_4)T\bar{v}(p_2) + \delta_{c_1,c_3}\delta_{c_2,c_4}\bar{u}(p_3) \times (i\gamma_5 T)u(p_1)[i\mathcal{D}_t^P(p_1 - p_3)]v(p_4)(i\gamma_5 T)\bar{v}(p_2), \tag{4}$$

$$-i\mathcal{M}_s = \delta_{c_1,c_2}\delta_{c_3,c_4}v(p_2)Tu(p_1)[i\mathcal{D}_s^S(p_1 + p_2)] \times v(p_4)T\bar{u}(p_3) + \delta_{c_1,c_2}\delta_{c_3,c_4}\bar{v}(p_2)(i\gamma_5 T) \times u(p_1)[i\mathcal{D}_u^P(p_1 + p_2)]v(p_4)(i\gamma_5 T)\bar{u}(p_3), \tag{5}$$

where $p_1(p_2)$ is the momentum of the incoming $q(\bar{q})$ and $p_3(p_4)$ that from the outgoing $q(\bar{q})$. The c_i are the color indices and T are the isospin projections on the mesons. $\mathcal{D}^S$ and $\mathcal{D}^P$ are the meson propagators of the form

$$\mathcal{D}^{S/P} = \frac{2G_S}{1 - 2G_S\Pi^{S/P}}, \tag{6}$$

with $\Pi^{S/P}$ being the polarization tensor in the scalar-pseudoscalar channel. This cross section is displayed in Fig. 3. We observe, as expected, almost everywhere an elastic cross section of the order of several millibarn. Close to the critical temperature ($T_c = 240$ MeV), however, the cross section increases dramatically due to the resonance structure in the s channel.

This resonance in the s channel dominates also the hadronization matrix elements close to the threshold whose Feynman diagrams are given in Fig. 4 with the matrix elements

$$-i\mathcal{M}_t = f_t\delta_{c_1c_2}\bar{v}(p_2)i\gamma_5 ig_1 S_F(p_1 - p_3)i\gamma_5 ig_2 u(p_1), \tag{7}$$

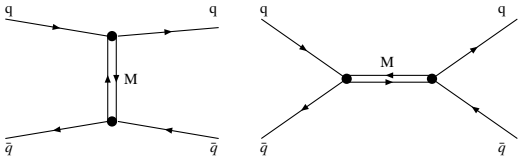

FIG. 2. Feynman diagrams of $q + \bar{q} \to q + \bar{q}$.

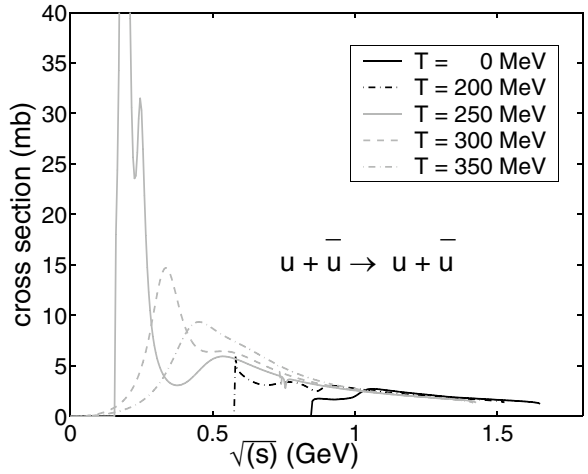

FIG. 3. Elastic cross section $\sigma_{u\bar{u}\to u\bar{u}}$ for different temperatures as a function of $\sqrt{s}$.

$$-i\mathcal{M}_u = f_u \delta_{c_1 c_2} \bar{v}(p_2) i\gamma_5 i g_1 S_F(p_1 - p_4) i\gamma_5 i g_2 u(p_1), \tag{8}$$

$$-i\mathcal{M}_s = \bar{v}(p_2)\delta_{c_1 c_2} f_s i\mathcal{D}(p_1 + p_2) \times \Gamma(p_1 + p_2; p_3) i g_1 i g_2 u(p_1). \tag{9}$$

We discuss here as an example the hadronization cross section for $u + \bar{u} \to \pi^+ + \pi^-$ (which has two s channels and one t channel) and the cross section for the inverse reaction, which are displayed in Fig. 5.

Around T_c the transition amplitude diverges close to the threshold; therefore the cross sections in both directions have their maximum there. The difference comes from the different flux and phase space factors.

Expanding plasma.—These cross sections suggest the following reaction scenario: as soon as projectile and target nuclei overlap, the density is high enough that the incoming nucleons overlap and partons can travel in this matter. By PQCD cross sections, which are of the order of some millibarn, the partons scatter, but these cross sections are not strong enough to equilibrate the system. While the system expands, the local available center of mass energy and hence the local temperature lower. The closer the system comes to the phase transition, the larger the elastic cross sections becomes. Because of this critical opacity, the system behaves more as a liquid then as a plasma close to

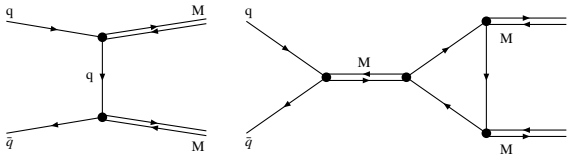

FIG. 4. Generic form of Feynman diagrams for the t and the s channel of $q + \bar{q} \to M + M$. The u channel is obtained by exchanging the mesons of the t channel.

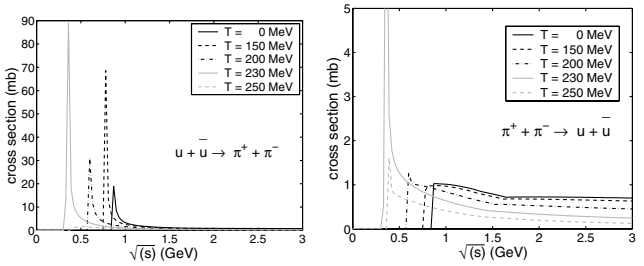

FIG. 5. Cross section for $u + \bar{u} \to \pi^+ + \pi^-$ and for the inverse reaction as a function of $\sqrt{s}$ for different temperatures.

the phase transition. In this phase the system approaches thermal equilibrium. The large cross sections during the expansion create in addition a large radial flow and—if the system is not isotropic in the azimuthal direction—also v_2 values. When passing the critical temperature, the large hadronization cross sections become effective because the created mesons do not decay anymore. The inverse cross section is small due to the kinematic conditions. The system cools locally and the maximum of the cross section moves to larger values of $\sqrt{s}$. This means that quark pairs with larger center of mass energies can now hadronize. During the expansion the local temperature passes from $T > T_c$ to 0. Therefore the cross sections are large for a large interval of $\sqrt{s}$, as seen in Fig. 6.

There remains the quantitative question of whether the strength of these cross sections is sufficient to hadronize the system completely: In order to check this we perform calculations using the quantum molecular dynamics approach [21], which has been successfully used to describe heavy ion reactions in this energy domain. In this approach, partons are presented as Gaussians whose centers in momentum and coordinate space follow Hamilton's equations. In addition, they interact via cross sections calculated from the same Hamiltonian. Figure 7 presents a model calculation for 30 quarks and 30 antiquarks and 100 pions initialized with isotropic distributions in coor-

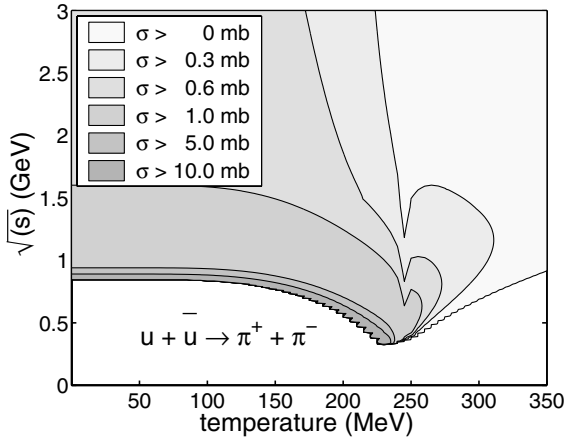

FIG. 6. Size of the cross section for $u + \bar{u} \to \pi^+ + \pi^-$ in the $\sqrt{s}$-temperature plane.

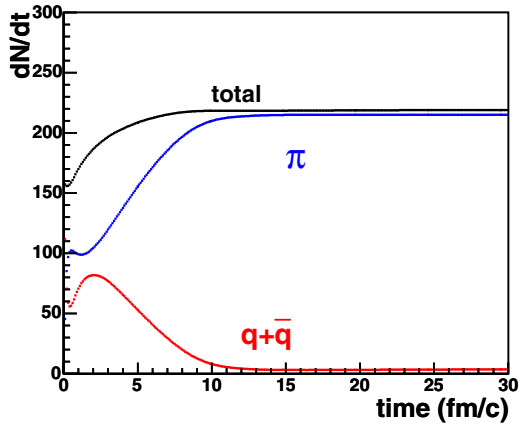

FIG. 7 (color online). Number of pions and quarks as a function of time.

dinate and momentum space for an energy density of 3 GeV/fm^3, which give a temperature slightly above T_c. There pions are unstable, and therefore the mesons can decay into the lighter quarks. When the system approaches the phase transition, the quark condensate $\langle q\bar{q}\rangle$ increases: the quarks become heavier and this energy is taken out from the relative motion. At the phase transition the mesons become stable and lighter than the quarks. They escape from the system in which the quarks remain (see Fig. 8). By emitting pions the remaining quark system cools down until finally only one quark and one antiquark are left which have not found a partner to created two pions. Thus, despite the fact that confinement is not enforced by the Lagrangian, under the condition of an expanding plasma confinement is almost complete.

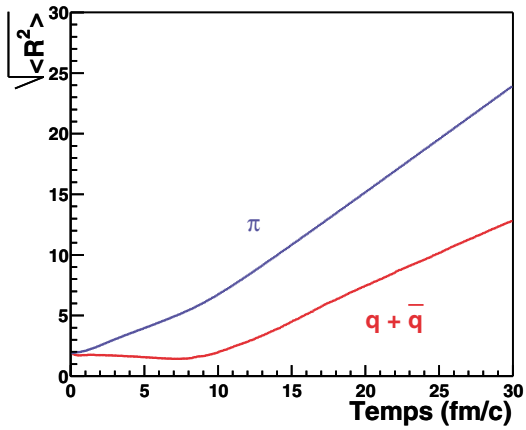

FIG. 8 (color online). Root mean square radius of the different species as a function of tome.

In conclusion, we have shown that the thermalization observed in the spectra in relativistic heavy ion reactions may be reconciled with the small PQCD cross section, assuming that the system passes a phase transition with critical opalescence during its expansion, as predicted by the NJL Lagrangian. Both elastic as well as inelastic cross sections become large over a large kinematic region which is covered by the expanding system and leads to a local thermalization as soon as the system comes to the phase transition. Because this transition takes places in an already expanding system, radial flow is created as observed experimentally. The observed v_2 values are an image of the asymmetry at the beginning of the expansion.

[1] T. Hirano, Phys. Rev. C **65**, 011901 (2002).
[2] D. Teaney, J. Lauret, and E. V. Shuryak, nucl-th/0110037.
[3] K. J. Eskola, H. Niemi, P. V. Ruuskanen, and S. S. Rasanen, Phys. Lett. B **566**, 187 (2003).
[4] P. F. Kolb and U. W. Heinz, Nucl. Phys. **A715**, 653 (2003).
[5] K. Morita, S. Muroya, C. Nonaka, and T. Hirano, Phys. Rev. C **66**, 054904 (2002).
[6] K. Adcox *et al.*, Phys. Rev. Lett. **89**, 082301 (2002).
[7] P. Houvinen, Nucl. Phys. **A715**, 299c (2003); *Quark-Gluon Plasma 3*, edited by R. C. Hwa and X.-N. Wang (World Scientific, Singapore, 2004).
[8] M. Thoma and M. Gyulassy, Nucl. Phys. **B351**, 491 (1991).
[9] X. N. Wang *et al.*, Phys. Rev. D **51**, 3436 (1995).
[10] K. Kajantie *et al.*, Phys. Rev. Lett. **59**, 2527 (1987).
[11] A. H. Müller, Nucl. Phys. **B572**, 227 (2000); Phys. Lett. B **475**, 220 (2000).
[12] J. Serreau, Nucl. Phys. **A715**, 805c (2003).
[13] D. Ebert, H. Reinhardt, and K. Volkov, Prog. Part. Nucl. Phys. **33**, 1 (1994).
[14] S. P. Klevansky, Rev. Mod. Phys. **64**, 649 (1992); Prog. Part. Nucl. Phys. **33**, 1 (1994).
[15] F. Gastineau, R. Nebauer, and J. Aichelin, Phys. Rev. C **65**, 045204 (2002).
[16] R. D. Pisarski and F. Wilczek, Phys. Rev. D **29**, 338 (1984).
[17] M. Alford, K. Rajagopal, and F. Wilczek, Phys. Lett. B **422**, 247 (1998).
[18] Z. Fodor and S. D. Katz, J. High Energy Phys. 03 (2002) 014; Nucl. Phys., Sect. B (Proc. Suppl.) **106**, 441 (2002).
[19] J. Hüfner, S. P. Klevansky, E. Quack, and P. Zhunag, Phys. Lett. B **337**, 30 (1994).
[20] P. Rehberg, S. P. Klevansky, and J. Hüfner, Phys. Rev. C **53**, 410 (1996).
[21] J. Aichelin, Phys. Rep. **202**, 233 (1991).